Vegetation Ecology and Diversity 63 (2026) e197154 | DOI 10.3897/ved.197154 Topical Collection

PENSOFT

VEGETATION ECOLOGY AND DIVERSITY

Research Article

UAV-based RGB imagery for assessing vegetation status in a Mediterranean area affected by *Xylella fastidiosa*[*]

Andrea Bertacchi[1], Diego Orazi[1], Sara Campigli[2], Guido Marchi[2], Lorenzo Drosera[3], Tiziana Lombardi[1]

1 *Department of Agricultural, Food and Agro-Environmental Sciences, University of Pisa, Pisa, Italy*

2 *Department of Agriculture, Food, Environment and Forestry, University of Florence, Firenze, Italy*

3 *Servizio Fitosanitario della Regione Toscana (SFR), Firenze, Italy*

Corresponding author: Tiziana Lombardi (tiziana.lombardi@unipi.it)

Academic editor: Gianmarco Tavilla ♦ **Linguistic editor:** Nicole Sebesta
Received 25 April 2026 ♦ **Accepted** 28 July 2026 ♦ **Published** 25 September 2026

Abstract

Vegetation monitoring in areas affected by plant pathogens is essential for assessing the vulnerability of plant communities and supporting the management of infected territories. Although field surveys remain the cornerstone of vegetation monitoring, RGB UAV technology is increasingly proving its value at local and regional scales for mapping plant communities and detecting diagnostic species of Annex I habitats. This study presents the results of a vegetation monitoring program carried out in 2021 and 2025 in a natural area of Monte Argentario (southern Tuscany, Italy), where *Xylella fastidiosa* subsp. *multiplex* ST87 has been spreading since 2018. Field surveys were integrated with UAV-based photogrammetric mapping and photointerpretation of ultra-high-resolution orthomosaics over a 2.5 ha polygon encompassing a mosaic of three Natura 2000 habitats (H9340, H5330, and H6220*). Multivariate analyses identified three floristically distinct assemblages corresponding to the main habitat types, and species-area analysis confirmed the representativeness of the sampling design. Comparing the two survey campaigns, the plant community showed remarkable compositional stability: species richness remained unchanged, and the minor increase in Shannon diversity reflected subtle shifts in relative dominance rather than any directional floristic change. Among the *Xylella* target species, *Cytisus laniger* showed a significant and counter-intuitive increase in cover, possibly reflecting a pre-symptomatic phase of infection or the intrinsic canopy expansion dynamics of this fast-growing resprouting shrub. The study establishes an important pre-symptomatic baseline for long-term monitoring of these habitats.

Keywords

Mediterranean shrubland, Natura 2000 habitats, UAVs, vegetation monitoring, *Xylella fastidiosa*

Introduction

Vegetation surveys have long been used to monitor ecosystems (Mueller-Dombois and Ellenberg 1974; Lengyel et al. 2008; ISPRA 2016). In addition to being the most widely used approach for vegetation classification, the phytosociological method has proven to be one of the most effective tools for monitoring plant communities and habitats (Godínez-Alvarez et al. 2009; Biondi et al. 2010; Kent 2012).

This applies both to surveys aimed at assessing anthropogenic impacts and transformations, and to investigations of damage caused by natural events, air pollution, and plant diseases (Gallet et al. 2010; Vacek et al. 2017; Konatowska and Rutkowski 2019; Bertacchi 2022; Vennin et al. 2025). In recent years, ground-based surveys have

[*] Topical Collection: "Advances in vegetation analysis through remote sensing technology".

Copyright *Andrea Bertacchi et al.* This is an open access article distributed under the terms of the Creative Commons Attribution License (CC BY 4.0), which permits unrestricted use, distribution, and reproduction in any medium, provided the original author and source are credited.

been gradually complemented by remote sensing observations which, depending on the spatial scale considered, range from satellite imagery to drone-based data (Turner et al. 2003; Fornace et al. 2014; de Castro et al. 2021).

UAV technology has proven especially valuable for surveying vegetation in difficult-to-reach areas, thanks to the high level of photographic detail achievable from aerial platforms, which allows remote recognition of different taxa (Strumia et al. 2020; Bertacchi et al. 2025).

When integrated with GIS systems, UAV platforms also enable precise quantification of species cover across vegetation patches (Chianucci et al. 2016; Quattrini et al. 2025; Bertacchi et al. 2026). Similarly, UAV technology is proving extremely useful in the fields of plant pathology detection and monitoring (Duarte et al. 2022; Perroy et al. 2022; Kouadio et al. 2023).

The present study followed the first detection of *Xylella fastidiosa* subsp. *multiplex* ST87 (hereinafter Xfm ST87) in Tuscany, recorded in November 2018 by the Regional Phytosanitary Service (hereinafter SFR) in the Municipality of Monte Argentario (GR) (Marchi et al. 2018). *Xylella fastidiosa* is a xylem-restricted bacterium naturally transmitted from plant to plant by insect vectors that feed on xylem fluids, primarily belonging to the families Aphrophoridae, Cercopidae, and Cicadellidae. The host range globally includes over 463 plant species distributed across 210 genera and 71 families (EFSA 2026). In some plant species, the progressive reduction in water flow within the vascular elements, caused by the accumulation of bacterial biofilm as well as by gums and tylose produced by the host, often leads to nonspecific symptoms of water deficiency that can easily be confused with those induced by other biotic and abiotic stress factors. During the early stages of colonization, leaf scorch, wilting, yellowing or bronzing, and premature leaf drop are commonly observed. Subsequently, twigs and branches of shrubs and trees begin to die back and, in some cases, the entire plant may die (EPPO 2020). Inexplicably, however, in the vast majority of its hosts, *Xylella fastidiosa* manages to proliferate without causing any apparent disease, thus behaving more like a commensal rather than a primary phytopathogen (Burbank and Roper 2021). Nevertheless, its introduction into new geographic areas followed by the fortuitous encounter with a new, highly susceptible host can have devastating consequences, as recently demonstrated by the outbreak of Olive Quick Decline Syndrome in Apulia (Italy) (Scortichini 2026). As a result, *Xylella fastidiosa* is currently included in the list of quarantine pests under European legislation (EU 2019/2072). In addition to the well-known threat posed to several agricultural crops and ornamentals including grapevine, citrus, coffee, oleander and olive (Sicard et al. 2018), concerns have also been raised about the potential risk to European forest and wild species (Desprez-Loustau et al. 2020).

In Corsica, Apulia and Tuscany, small trees or shrubs typical of the Mediterranean maquis, such as *Rhamnus* or *Cistus*, were reported among hosts of *Xylella fastidiosa* (Denancé et al. 2017; EFSA 2019; Saponari et al. 2019; Falsini et al. 2025).

Since 2018, Xfm ST87 has spread throughout much of the Monte Argentario territory, primarily in the two coastal areas to the north and south of the promontory. From 2018 to the present, of the 175 taxa sampled, 29 (16.5%) have tested positive at least once. Some of the wild species characteristic of the Monte Argentario habitats have proven to be particularly susceptible to the pathogen: common broom (*Spartium junceum* L., Fabaceae), hairy thorny broom (*Cytisus laniger* DC., Fabaceae), buckthorn (*Rhamnus alaternus* L., Rhamnaceae) and white rockrose (*Cistus monspeliensis* L., Cistaceae). These species are widely distributed throughout the territory examined and were considered target species in the SFR sampling and monitoring to delimit infected and buffer zones. It should be noted that to date, the olive tree (preferential host in Puglia for the ST53 of *pauca* subspecies) has never been found infected with Xfm ST87 (SFR 2026).

Among the questions that the SFR asked itself in establishing a strategy for controlling, delimiting and, possibly, eradicating the pathogen from the territory of Monte Argentario, was to somehow determine the danger of the pathogen to the conservation of the natural habitats present in this territory in their vegetational component. This is largely determined by the impact that phytopathologies can have on natural plant communities (Gilbert 2002; Burdon et al. 2006).

For this reason, monitoring activities on the vegetation component of a sample area of Monte Argentario began in 2021, based on drone surveys and followed by field surveys; this investigation presents the first findings on the potential impact of Xfm ST87 on phytocoenoses that are characteristic of Monte Argentario's habitats.

Material and methods

Study area

Monte Argentario is a coastal promontory located in southwestern Tuscany, central Italy (42.399339°N, 11.154622°E) (Fig. 1). Although orographically isolated from the mainland, it is connected to the Tuscan coast by two sandy tombolos and an internal lagoon system (Lazzarotto et al. 1964). The promontory covers approximately 60 km^2 and is characterized by steep rocky cliffs and rugged topography, reaching 635 m a.s.l. at Punta Telegrafo.

Geologically, the area exhibits a complex assemblage of limestone and dolostone, metasandstone, acid metavolcanic rock, calcschist, and metamorphic ophiolite (Carmignani and Lazzarotto 2004), while the climate is Mediterranean (Csa type: hot-summer Mediterranean climate; Köppen 1936), with mild winters and hot, dry summers (Arrigoni and Di Tommaso 1997).

Bioclimatically, the area falls within the Mediterranean macrobioclimate (pluviseasonal-oceanic variant), spanning a gradient from the lower mesomediterranean thermotype at coastal elevations to the upper

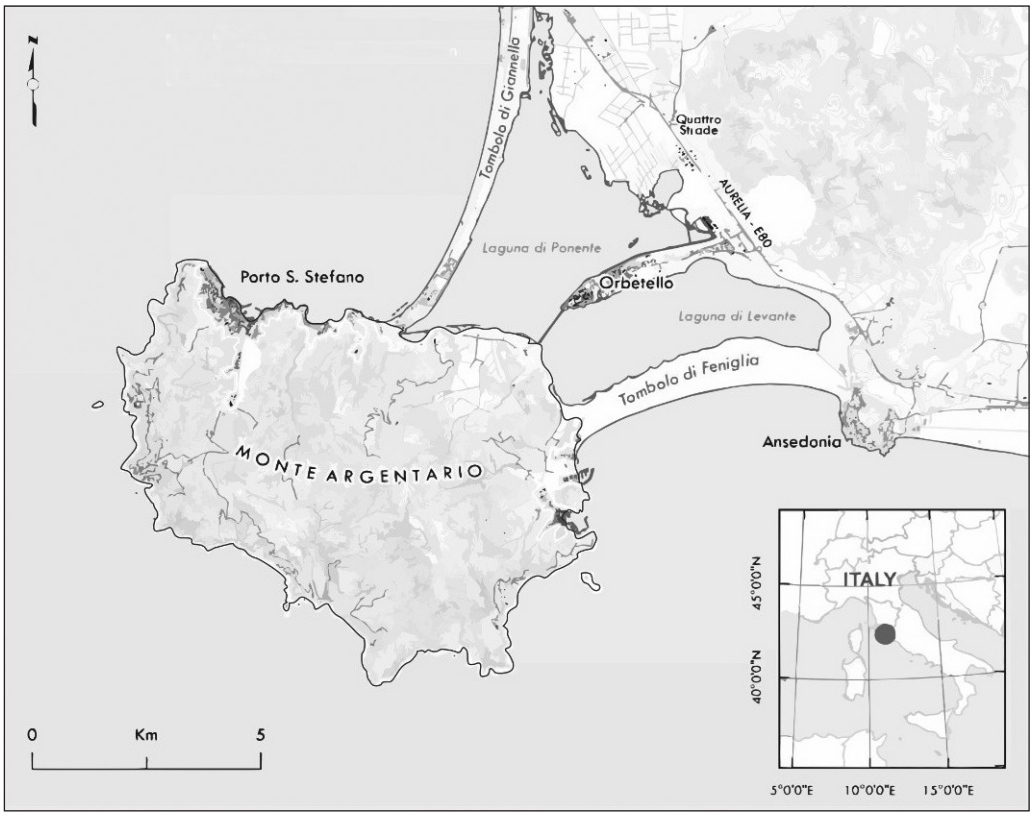

Figure 1. Geographical location of the Monte Argentario promontory (southern Tuscany, Italy).

mesomediterranean thermotype towards the summit (Pesaresi et al. 2017), within the Mediterranean Biogeographic Region (European Environment Agency 2017).

The vascular flora of Monte Argentario includes approximately 1200 taxa. The biological spectrum (Raunkiaer 1934) shows a predominance of therophytes (40%), followed by hemicryptophytes (30%), and geophytes (15%). This pattern, together with the prevalence of Mediterranean, East-Mediterranean, and Atlantic-Mediterranean chorotypes confirms the strictly Mediterranean character of the area (Baldini 1995).

The structure of the vegetation is a dynamic mosaic of sclerophyllous evergreen forests and their degradation stages, including Mediterranean shrubland, garrigues, and discontinuous annual grasslands. This mosaic reflects long-term anthropogenic influence (agriculture, grazing, recurrent fires, and land abandonment) superimposed on natural successional processes.

Phytosociologically, these communities can be framed within the classes *Quercetea ilicis* Br.-Bl. ex A. Bolòs y Vayreda 1950, *Querco-Fagetea* Br.-Bl. and Vlieger in Vlieger 1937, and *Festuco-Brometea* Br.-Bl. and Tx. ex Br.-Bl. 1949 (Arrigoni and Di Tommaso 1997).

Thirteen habitat types listed in Annex I of the EU Habitats Directive (92/43/EEC) have been identified in the area (Viciani et al. 2018).

The most representative habitats are:

- Habitat 9340: *Quercus ilex* and *Quercus rotundifolia* forests (~2000 ha);
- Habitat 5330: Thermo-Mediterranean and pre-desert scrub (~1000 ha);
- Habitat 6220*: Pseudo-steppe with grasses and annuals of the *Thero-Brachypodietea* (~506 ha).

Habitats 5330 and 6220* frequently form intricate mosaics representing dynamic successional or degradation stages. Abandoned olive groves (~700 ha) are currently progressing towards Habitat 5330. In addition, approximately 1200 ha are occupied by active agricultural land and 600 ha by urban areas and infrastructure.

Field surveys and UAV technology

The study was conducted in the Valle della Soda area, a north–south oriented valley located in the northern sector of Monte Argentario (Tuscany, Italy). A 2.5 ha study polygon was delineated to include the valley bottom (impluvium) and adjacent slopes, encompassing the main habitat mosaic present in the area (Natura 2000 habitats 9340, 5330 and 6220*) (Fig. 2a, b); the site falls within the officially designated "demarcated area" according to EU Regulation 2020/120 (Article 4).

To determine the presence or absence of *Xylella fastidiosa* subsp. *multiplex* ST87 (Xfm ST87) in the study site, annual surveys, from 2021 to 2025, were carried out following EFSA and EPPO guidelines (EFSA 2023; EPPO 2023) and in accordance with the Commission Implementing Regulation (EU) 2020/1201. The area spans an

elevational gradient from 130 to 240 m a.s.l., allowing the inclusion of structurally heterogeneous vegetation types within a limited spatial extent. An integrated field–UAV surveys approach was adopted.

In May–June 2021, a complete floristic survey of the study area was conducted to document the species pool of the site. In the same period, vegetation surveys were performed within permanent plots. Twelve permanent plots were established to sample the habitat mosaic occurring within the study area. Plot size was defined according to physiognomy: 10 × 10 m in tree-dominated stands and 5 × 5 m in shrub- and herb-dominated stands. Plots were georeferenced and permanently recorded to ensure precise relocation during the second survey campaign in 2025 (Fig. 2c ; Suppl. material 1: table S3). The same plots were resurveyed in June–July 2025 under comparable phenological conditions.

Field surveys allowed confirmation of the taxonomic identification of species recognizable on the orthomosaics and the recording of taxa not detectable from aerial imagery due to canopy overlap, small size, or chromatic similarity. Species cover within each plot was quantified through mapping on ultra-high-resolution RGB orthomosaics derived from UAV imagery, allowing precise spatial delineation of vegetation patches without relying on visual field estimates.

Botanical nomenclature follows Bartolucci et al. (2024) and subsequent updates provided by the Portal to the Flora of Italy (Martellos et al. 2020). Biological life forms and chorological types were assigned following Pignatti et al. (2017–2019). Diagnostic species for Annex I habitats (Directive 92/43/EEC) were specifically recorded to support habitat attribution and vegetation classification.

UAV surveys were conducted in both vegetation-sampling years using different UAV platforms. In 2021, flights were performed with a DJI Phantom 4 Pro equipped with a 20 MP RGB sensor (1" CMOS; 24 mm equivalent focal length). In 2025, surveys were conducted using a DJI Mini 4 Pro equipped with a 48 MP RGB sensor (1/1.3" CMOS; 24 mm equivalent focal length). Automated flight missions were programmed at a constant elevation of 25 m above ground level, with 60% forward overlap and 80% side overlap. Based on flight elevation and sensor geometry, the theoretical Ground Sampling Distance (GSD) was approximately 0.68 cm/pixel for the Phantom 4 Pro and 0.44 cm/pixel for the Mini 4 Pro under ideal geometric conditions. A summary of the UAV survey parameters for both campaigns is provided in Table 1.

No ground control points (GCPs) were deployed; georeferencing relied on the onboard GNSS system of the UAVs. Given the limited spatial extent of the study area (2.5 ha), the ultra-high spatial resolution of the imagery, and the plot-based analytical framework, relative spatial consistency between survey years was considered sufficient for accurate intra-plot comparisons.

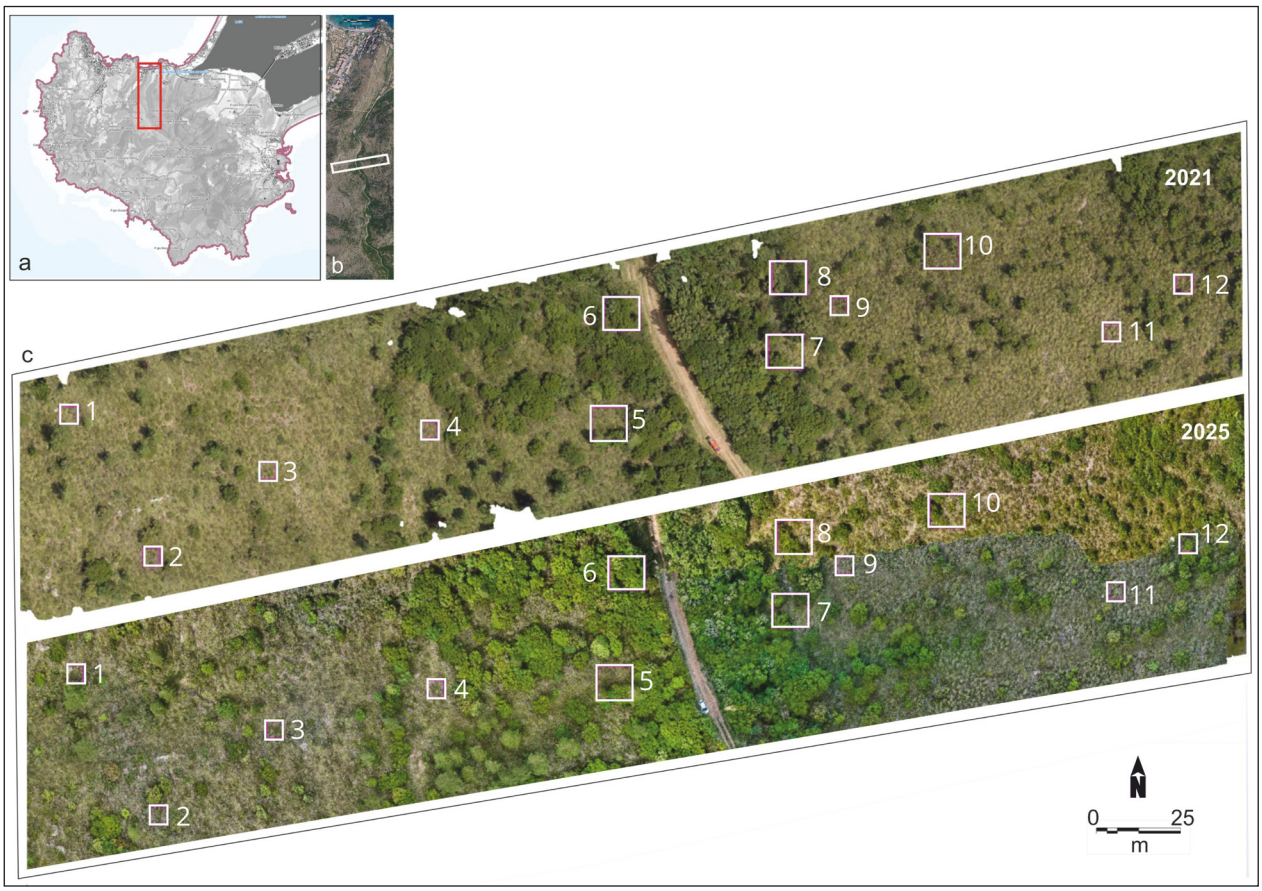

Figure 2. Localization on Monte Argentario of the survey site (**a** and **b**) and drone orthophotomosaic (**c**) of the sample area with the overlapping plots.

Table 1. Summary of the UAV survey workflow (2021 and 2025 campaigns).

Parameter	2021 survey	2025 survey
Platform	DJI Phantom 4 Pro	DJI Mini 4 Pro
Sensor	20 MP RGB, 1" CMOS, 24 mm equiv.	48 MP RGB, 1/1.3" CMOS, 24 mm equiv.
Ground Sample Distance (GSD)	≈ 0.68 cm/pixel	≈ 0.44 cm/pixel
Flight elevation	25 m AGL	
Overlap	60% forward / 80% side	
Exposure settings	Automatic exposure, fixed white balance	
Orthomosaic software	Agisoft Metashape Professional v. 1.7.5	
Delineation method	Manual (human-operator photointerpretation)	

Flights in both years were conducted under stable weather conditions, with clear or slightly hazy skies, no precipitation, and low wind speed (< 5 m/s), to minimize motion blur and illumination variability. Missions were carried out between 10:30 and 14:30 local time to ensure high solar elevation and reduced shadow effects. Camera settings were maintained consistent across flights using automatic exposure and fixed white balance to minimize chromatic variability between survey years.

Image alignment, dense point cloud generation, orthomosaic production, and 3D reconstruction were performed in Agisoft Metashape (v. 1.7.5) (Agisoft LLC 2021) (Fig. 3). Model quality was assessed using the reprojection Root Mean Square Error (RMSE), which averaged 0.29 pixels. Orthomosaics were georeferenced in WGS 84/UTM zone 32N (EPSG: 32632) and analyzed in QGIS 3.42.0.

Within each permanent plot, species cover was quantified through the manual delineation of individual taxa on ultra-high-resolution RGB orthomosaics, performed by a human operator.

Only species previously recorded and taxonomically confirmed during field surveys were mapped. Field observations conducted in both years were used to validate species presence and support image-based delineation, thereby reducing misclassification among morphologically similar taxa. Mapping focused primarily on dominant or structurally distinguishable species exhibiting consistent canopy texture or chromatic patterns. Absolute cover values (m^2) were converted into percentage cover as (species area / plot area) × 100, allowing direct interannual comparison (2021–2025).

Data analysis and processing

To assess the spatial distribution of plant species and validate the adequacy of the sampling effort, the Species-Area Relationship (SAR) (Tjørve and Tjørve 2017) was modelled using the Arrhenius power function ($S = c\ A^z$), where S is the number of species, A is the area, c is a constant representing the expected richness per unit area, and z represents the species accumulation rate (Arrhenius 1921).

The SAR was fitted using a log-log linear regression on 13 data points, comprising the 12 permanent plots individually (areas of 0.0025 ha for shrub- and herb-dominated stands and 0.01 ha for tree-dominated stands, with species richness recorded during the 2021 survey) and the total study polygon (2.5 ha, with the total number of species recorded through the complete floristic survey conducted in 2021). The Arrhenius power function $S = c \cdot A^z$ was linearized by log-log transformation for regression fitting, with the *z*-value estimated as the slope of the ordinary least squares regression and *c* derived from the intercept.

It should be noted that the plot-scale areas correspond to spatially non-contiguous permanent plots rather than nested sampling units, and that the two plot sizes reflect differences in vegetation physiognomy rather than a systematic area gradient. The resulting exponent therefore reflects scaling between individual sampling units and landscape extent rather than a classical nested-area design, and direct comparisons with *z*-values derived from strictly nested designs should be made with caution.

Additionally, to test the ecological plausibility of the observed richness, the expected number of species at the landscape scale was independently calculated using literature-based *z*-values typical for Mediterranean shrublands (Drakare et al. 2006; Tjørve 2009).

Data structure and transformation

Vegetation data were organized as a species × plot matrix using percentage cover values recorded in 2021 and 2025. To evaluate potential temporal shifts in community composition, analyses were conducted on square-root transformed cover data (Legendre and Gallagher 2001). The square-root transformation was applied to reduce the disproportionate influence of highly dominant taxa, particularly *Ampelodesmos mauritanicus*, which structurally characterizes parts of the study area. This transformation allowed greater sensitivity to change in subdominant and shrub-layer species.

Hierarchical clustering

Floristic–vegetational patterns among permanent plots were explored through hierarchical cluster analysis. Species cover values were square-root transformed to reduce the influence of dominant taxa while preserving relative abundance structure. Dissimilarity between plots was

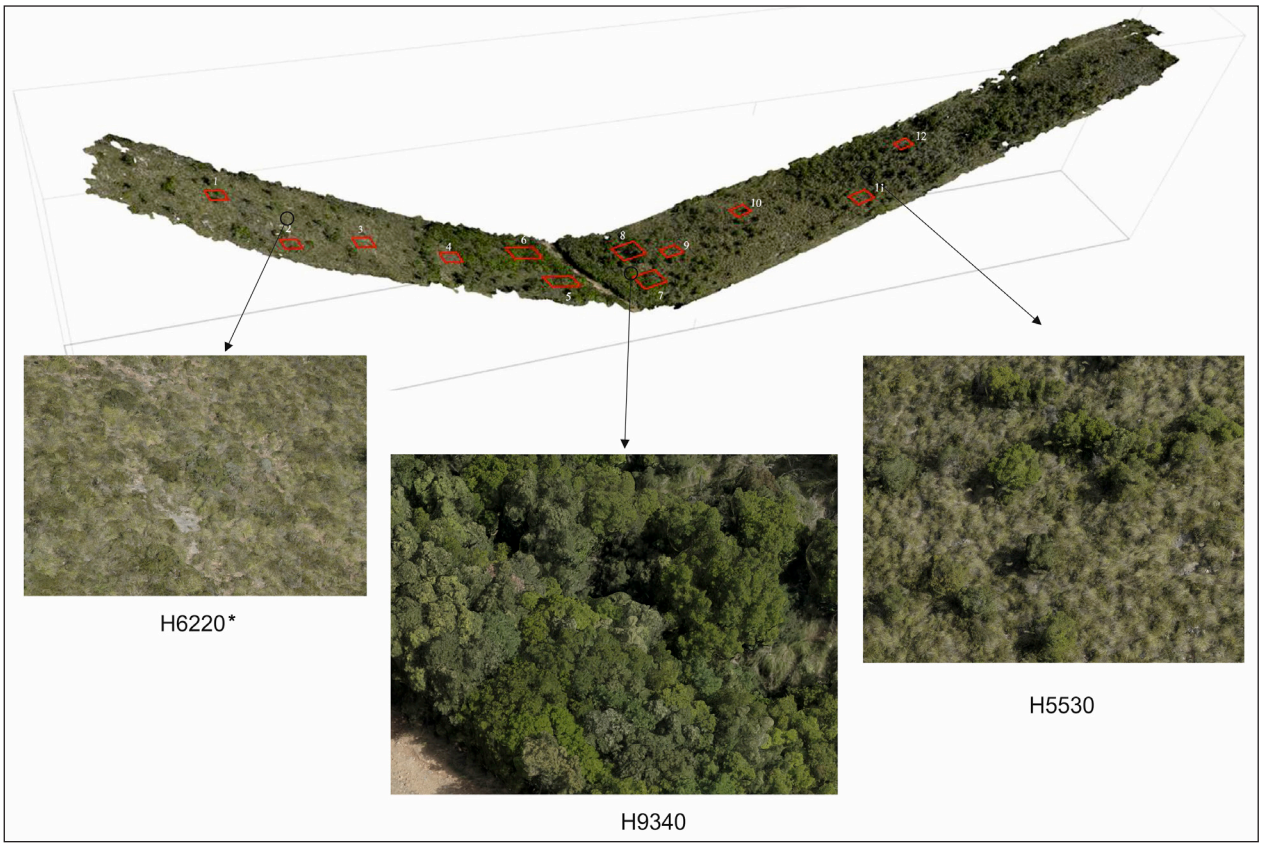

Figure 3. 3D reconstruction of the sample area and restitution of the three habitat types.

calculated using the Bray–Curtis index, which is widely recommended for ecological community data due to its sensitivity to compositional differences and its robustness to joint absences (Legendre and Legendre 2012).

Agglomerative hierarchical clustering was performed using the unweighted pair-group method with arithmetic mean (UPGMA; average linkage). The resulting dendrogram was visually inspected and subsequently partitioned into alternative cluster solutions (k = 2 and k = 3) to explore primary and secondary compositional structures. Cluster boundaries were identified by examining the distribution of fusion heights in the dendrogram. All multivariate analyses were conducted using the Bray–Curtis dissimilarity matrix derived from transformed cover data.

Alpha-diversity analysis

To evaluate temporal changes in local plant biodiversity, alpha-diversity was assessed for each permanent plot by calculating Species Richness (S), the Shannon Diversity Index (H') (Shannon 1948), Simpson's Index (1−D) (Simpson 1949), and Pielou's Evenness (J') (Pielou 1966). Species richness was defined as the total number of vascular plant species recorded per plot. Shannon diversity was calculated as: $H' = -\Sigma\, p_i \ln(p_i)$ where p_i represents the proportional cover of species i within each plot. All indices were calculated from raw percentage cover values, consistently with standard alpha-diversity practice. To account for the repeated-measures design of the permanent plots, differences in alpha-diversity metrics between the first survey (2021) and the resurvey (2025) were assessed using the Wilcoxon signed-rank test because the data were not normally distributed.

Ordination analysis (PCoA) and PERMANOVA

To visualize floristic gradients and assess the spatio-temporal dynamics of the plant communities, unconstrained ordination was performed using Principal Coordinates Analysis (PCoA). The ordination was based on the same Bray–Curtis dissimilarity matrix applied in the hierarchical clustering, derived from square-root transformed species cover data. PCoA was performed to visualize multivariate differences among plots and sampling years in reduced ordination space. Temporal separation was assessed by inspecting clustering patterns along the first two principal coordinate axes.

To test for statistically significant differences in species composition, a Permutational Multivariate Analysis of Variance (PERMANOVA; Anderson 2001) was conducted. For PERMANOVA, pseudo-F statistics, R^2 values, and p-values were reported.

To test for temporal changes in community composition, Year (2021 vs. 2025) was used as the explanatory factor. To account for the repeated-measures design of the permanent plots, permutations were constrained within each Plot ID (used as a block/stratum), ensuring that the temporal effect

was tested within the same spatial units. A total of 9999 permutations was specified. A complementary PERMANOVA model including Plot as an explicit factor was also fitted to quantify spatial structuring among permanent plots. Cluster membership derived from hierarchical clustering was used for descriptive interpretation of vegetation assemblages and was not included as an explanatory factor in the PERMANOVA models. Homogeneity of multivariate dispersion among years was evaluated using PERMDISP (Anderson 2006) to ensure that significant PERMANOVA results, if detected, were attributable to shifts in centroid location rather than differences in within-group variability.

Species contribution (SIMPER)

Similarity Percentage (SIMPER) analysis (Clarke 1993) was performed to identify the species contributing most to the average Bray–Curtis dissimilarity between surveys conducted in 2021 and 2025. The analysis was applied to square-root transformed species cover data, consistent with the transformation used for distance-based multivariate analyses.

SIMPER decomposes the overall between-group dissimilarity into the contribution of individual species by calculating the average contribution of each taxon to the Bray–Curtis distance between groups. Species contributions were expressed both as absolute average dissimilarity and as percentage contribution to total between-year dissimilarity. Cumulative contributions were used to identify the set of taxa accounting for the majority of interannual compositional differences.

Software

Flight missions were planned and executed using the DJI Fly® application (DJI 2024). UAV images were processed through a photogrammetric workflow in Agisoft Metashape Professional® (64 bit) to generate dense point clouds and orthomosaics.

Spatial analyses, vegetation interpretation, and cartographic outputs were performed using QGIS (version 3.42.0) (QGIS Development Team 2024).

Statistical analyses were conducted in R (R Core Team 2024), and community-level metrics were calculated using the vegan package (Oksanen et al. 2023).

The vegetation dataset supporting the results of this study is available as Supplementary material (Suppl. material 1: table S2).

Results

Xfm ST87 detection in the study site

During the monitoring, 34 taxa were analyzed as a whole, comprising a total of 454 samples. The presence of Xfm ST87 in the study site could be confirmed in each year, although estimated annual incidence varied considerably: the lowest was in 2022 (0.062), when the sampling effort was greatest (192 analyzed), and the highest was in 2024 (0.186), when 43 plants were analyzed. This variation in sampling efforts reflects both the need, in the early years, to test a broader range of plant species in order to identify those in which the bacterium could most easily be detected by PCR, and the specific aim of this monitoring, namely to confirm the consistent presence of the pathogen over time rather than to quantify its prevalence within the study area (Suppl. material 1: fig. S1).

Floristic composition

A total of 90 vascular plant species were recorded within the study area, including both the permanent survey plots and the surrounding area (Suppl. material 1: table S1).

The overall floristic composition reflects the Mediterranean sclerophyllous vegetation framework typical of Natura 2000 Habitat 5330 (Thermo-Mediterranean and pre-desert scrub), with localized structural elements referable to Habitat 9340 (*Quercus ilex* forests).

Habitat 6220* (Pseudo-steppe with grasses and annuals of the *Thero-Brachypodietea*) occurs in small patches within the broader landscape matrix but is only marginally represented within the sampled permanent plots (Suppl. material 1: table S2).

The biological spectrum highlights a strong structural dominance of woody life forms, reflecting the physiognomy of the local habitats. Phanerophytes (including nanophanerophytes) constitute the most abundant life form, accounting for 58.9% of the total flora, followed by hemicryptophytes (13.3%), chamaephytes (11.1%), and therophytes (11.1%).

From a phytogeographical perspective, Mediterranean chorotypes dominate the assemblage (63.3% of species), including 44.4% Steno-Mediterranean and 18.9% Euri-Mediterranean elements. Eurasian and paleotemperate chorotypes represent a minor fraction (13.3%), mainly linked to the shadier understory conditions of Habitat 9340 or localized mesic microhabitats.

UAV imagery integrated with GIS-based spatial analysis was employed to quantify absolute and relative ground cover and to assess diachronic changes between 2021 and 2025 (Suppl. material 1: fig. S2).

Field surveys remained essential for the accurate identification of most herbaceous species and small shrub or tree seedlings. Drone imagery proved fully reliable for larger shrub and arboreal taxa.

Within the permanent plots monitored in 2021 and 2025, a total of 43 species were identified (Suppl. material 1: table S2).

Vegetation is primarily composed of two dominant taxa showing the highest cover and frequency values: *Ampelodesmos mauritanicus* (mean cover 37%; 100% frequency) and *Erica multiflora* (mean cover 14%; 80% frequency), confirming the prevalence of shrub–grass typical of Habitat 5330.

Species–area relationship (SAR)

A log-log linear regression of species richness against area was applied across the 13 data points (12 permanent plots and the total study polygon) to estimate the general species accumulation trend ($R^2 = 0.886$, $p < 0.001$). The estimated scaling exponent was $z = 0.299$ (± 0.032 SE) and the intercept parameter $c = 63.49$, giving the species–area function:

$$S = 63.49 \times A^{0.299}$$

(with A expressed in hectares).

Given the non-nested structure of the design (see Methods), these statistics should be interpreted in light of their primary purpose: assessing whether the observed species richness of 90 taxa at 2.5 ha is ecologically consistent with theoretical expectations.

The observed value is broadly consistent with the model prediction (S = 83.5) and falls within the range predicted from literature-based *z*-values for continuous Mediterranean vegetation ($z = 0.15–0.25$; predicted range: 73–80 species), supporting the adequacy of the sampling design (Suppl. material 1: fig. S3).

Vegetation hierarchical cluster analysis

Cluster analysis applied to vegetation survey data identified three compositional assemblages (Cluster A, Cluster B and Cluster C) within the study area (Suppl. material 1: table S2; Fig. 4). At a Bray-Curtis dissimilarity threshold of approximately 0.54, the dendrogram clearly resolves these three distinct groupings, indicating meaningful floristic differentiation within the sampled vegetation mosaic.

Cluster A (Plot 6, 7, and 8) is characterized by higher cover of woody sclerophyllous taxa including *Arbutus unedo*, *Pistacia lentiscus*, *Erica arborea*, and *Quercus ilex*, species diagnostic to Habitat 9340.

Cluster B (Plot 1–5, 9, 11, and 12) encompasses the majority of surveyed plots and is dominated by *Ampelodesmos mauritanicus*, *Erica multiflora*, *Cytisus laniger*, and various *Cistus* species, diagnostic to Habitat 5330.

Cluster C (Plot 10) captures a subgroup floristically and physiognomically attributable to an intermediate vegetation type between Habitats 5330 and 9340.

Cluster analysis consistently grouped surveys conducted within the same plot in 2021 and 2025 into paired subclusters. Each 2021 survey clustered with its corresponding 2025 survey, indicating strong compositional consistency between the two survey campaigns. Observed interannual differences were limited to minor shifts in relative dominance among co-occurring woody species, with no evidence of directional floristic change.

Alpha-diversity patterns

Species richness (S), Shannon Diversity (H'), Simpson's Index (1–D), and Pielou's Evenness (J') were compared between 2021 and 2025 using Wilcoxon signed-rank paired tests to account for the repeated-measures design (n = 12 plots).

Species Richness (S) did not differ significantly between years (Wilcoxon signed-rank test, $W = 5.0$, $p = 0.750$). The Shannon Diversity Index (H') showed a marginal numerical variation, shifting from a mean of 1.690 (± 0.327 SD) in 2021 to 1.711 (± 0.343 SD) in 2025 ($W = 13.0$, uncorrected $p = 0.043$).

Similarly, Simpson's Index (1–D) and Pielou's Evenness (J') displayed positive trends just below the significance threshold (1–D: $W = 15.0$, $p = 0.064$; J': $W = 16.0$, $p = 0.077$). As median and interquartile ranges were broadly comparable between survey years (Fig. 5), these subtle fluctuations represent microscopic adjustments in relative species abundances rather than robust structural changes, confirming the overall stability of local alpha-diversity over the study period.

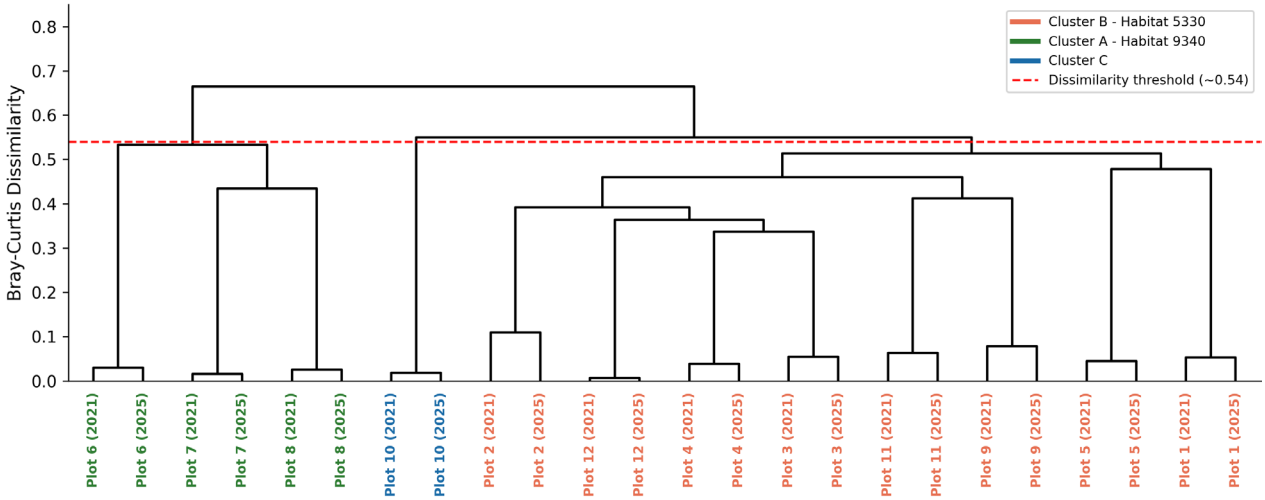

Figure 4. Hierarchical clustering of vegetation plots based on Bray–Curtis dissimilarity calculated on square-root transformed species cover data, using UPGMA linkage. The red dashed line indicates the dissimilarity threshold used to identify major clusters corresponding to different vegetation types (see text for details).

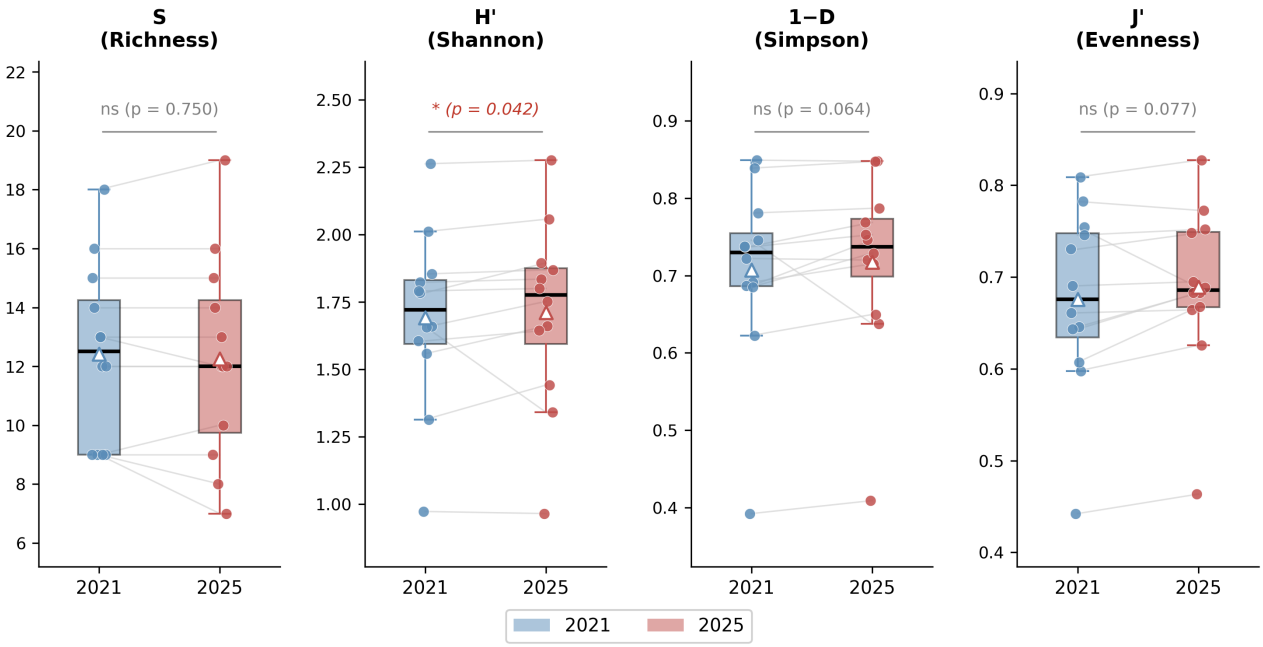

Figure 5. Temporal variations in alpha-diversity within the monitored permanent plots (n = 12). Boxplots display the median and interquartile ranges for Species Richness (S), Shannon Diversity Index (H'), Simpson's Index (1−D), and Pielou's Evenness (J') recorded in 2021 and 2025. Individual plot values are represented by dots, with lines connecting paired observations from the same plot. Wilcoxon signed-rank tests indicated no significant change in S ($p = 0.750$), a significant increase in H' ($p = 0.043$), and non-significant positive trends for 1−D ($p = 0.064$) and J' ($p = 0.077$).

Ordination analysis (PCoA) and PERMANOVA

The first two axes explained 41.8% and 16.4% of the total variation, respectively (58.2% cumulative). Ordination revealed strong overlap between sampling years, with each permanent plot maintaining close spatial proximity to its corresponding resurvey. No consistent directional displacement between years was evident along the main ordination axes, and paired surveys clustered tightly in multivariate space.

To formally test temporal effects while accounting for the repeated-measures design, a PERMANOVA was performed with permutations constrained within plots (strata = Plot). The analysis detected a statistically significant effect of Year (Pseudo-$F = 0.087$; $p = 0.007$). However, the explained variance associated with the temporal factor was extremely low ($R^2 = 0.0039$), indicating that Year accounted for less than 0.4% of total compositional variability (Fig. 6).

A complementary model including Plot as an explicit factor confirmed significant spatial structuring among plots ($R^2 \approx 0.995$; $p < 0.001$), whereas the marginal contribution of Year remained negligible.

No significant differences in dispersion between years were detected ($F = 0.0011$; $p = 0.972$), indicating comparable within-group variability and excluding dispersion-driven effects in the PERMANOVA results.

Collectively, multivariate analyses indicate strong spatial differentiation among plots and minimal temporal compositional change between 2021 and 2025.

SIMPER analysis

Although the overall interannual dissimilarity was low and the temporal effect negligible in PERMANOVA terms ($R^2 = 0.0039$), SIMPER analysis was performed to identify which species, and in particular which *Xylella fastidiosa* target species, contributed most to the observed between-year compositional differences. This information is directly relevant to the phytosanitary monitoring objectives of the study, as it allows assessment of whether the minimal floristic change detected was concentrated in susceptible taxa or distributed diffusely across the community.

Overall interannual dissimilarity was low, consistent with the limited variance explained by Year in PERMANOVA. The highest individual contributions to between-year dissimilarity were associated with *Cytisus laniger* (36.3%), followed by *Brachypodium sylvaticum* (11.6%), *Erica multiflora* (8.3%), and *Cistus monspeliensis* (6.5%) (Fig. 7). Notably, *Cytisus laniger*, the Xfm ST87 target species showing the most marked cover increase over the monitoring period, accounted alone for over one third of total interannual dissimilarity, reflecting its floristic dynamism within an otherwise stable community. The remaining target species (*Spartium junceum*, *Rhamnus alaternus*, *Cistus monspeliensis*) contributed marginally and showed no directional change. Between-year dissimilarity was otherwise distributed diffusely across common perennial taxa, with no single non-target species accounting for a disproportionate share of variation.

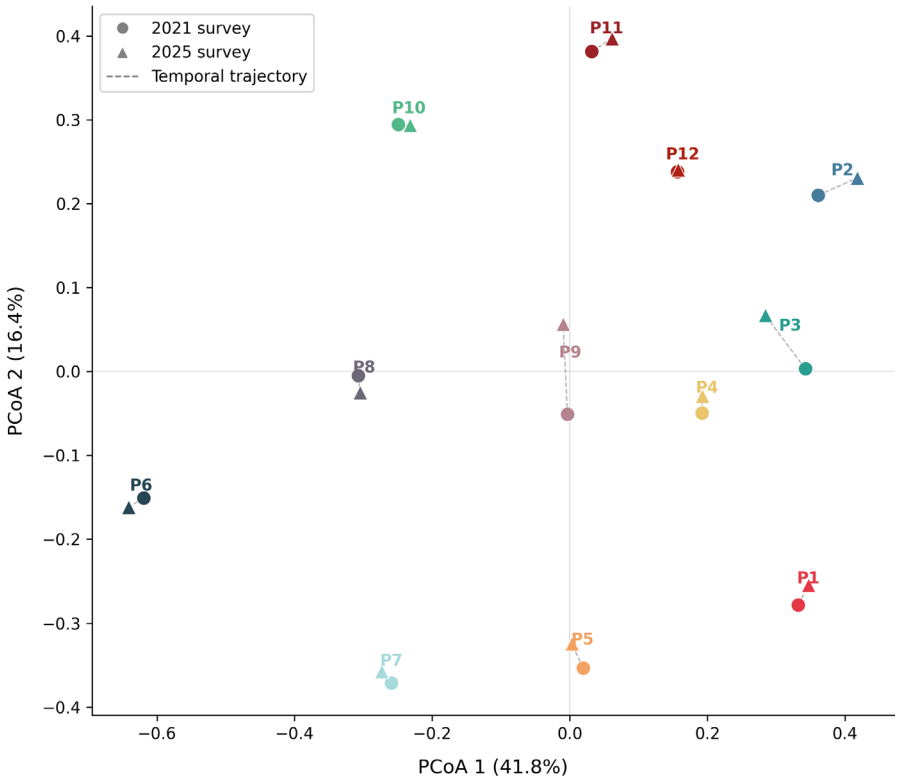

Figure 6. Principal Coordinates Analysis (PCoA) ordination based on Bray–Curtis dissimilarity of square-root transformed species cover data. Symbols represent the individual vegetation surveys, with circles indicating the baseline sampling in 2021 and triangles representing the 2025 resurveys. Different colors identify the 12 permanent plots (P1–P12). Dashed lines connect paired observations from the same plot, visualizing their temporal trajectories over the study period. The exceptionally short trajectories and the strong overlap between years highlight the high compositional stability and structural inertia of the plant communities. In contrast, the spatial separation of the plots across the ordination space reflects the strong underlying habitat heterogeneity.

Discussion

Floristic richness and biological spectrum

The total vascular flora recorded in the Valle della Soda study area, 90 species over a 2.5 ha polygon, reflects the floristic richness expected for well-preserved Mediterranean maquis and garrigue mosaics of the Tyrrhenian coast. The dominance of Steno-Mediterranean and Euri-Mediterranean chorotypes (63.3% combined) is consistent with the biogeographic positioning of Monte Argentario within the Mediterranean Biogeographic Region and aligns with the phytosociological framework of the *Quercetea ilicis* class, which characterizes the sclerophyllous evergreen vegetation of the central-western Mediterranean basin (Blasi et al. 2010; Biondi et al. 2014). The strong prevalence of phanerophytes (58.9%), with therophytes accounting for only 11.1% of the total flora, indicates a structurally mature community at a shrubland-to-woodland transitional stage, little affected by recent large-scale disturbances such as fire or intensive grazing. The very low therophyte cover within permanent plots (below 1%) reinforces this interpretation, as annual species tend to expand under post-disturbance or soil-degradation conditions in Mediterranean ecosystems (Lloret et al. 2005).

Species-area relationship: sampling adequacy and structural interpretation

The species-area scaling exponent obtained (z = 0.299 ± 0.032 SE, R^2 = 0.886, p < 0.001) falls within the theoretical range proposed for continuous, non-isolated continental ecosystems (z = 0.15–0.30; Rosenzweig 1995), and is consistent with values reported for Mediterranean shrubland and semi-natural vegetation systems (Drakare et al. 2006; Tjørve 2009), albeit at the upper boundary of this interval. The high goodness of fit confirms that the Arrhenius power function adequately describes species accumulation across the sampled spatial extents, from individual plots to the full study polygon. This value is also fully coherent with the physiognomic and structural characteristics of the Habitat 5330-dominated mosaic: as demonstrated by Keeley and Fotheringham (2003), shrub-dominated communities characterized by a dense matrix of perennial woody species and a low occurrence of annuals typically exhibit stable and relatively low z-values — precisely the pattern observed here, where phanerophytes and chamaephytes account for nearly 70% of the biological spectrum while therophytes are marginally represented.

The exponent obtained is slightly higher than broader Italian baseline estimates (z ≈ 0.26) (D'Antraccoli et al. 2024). Rather than reflecting a scale-dependent damp-

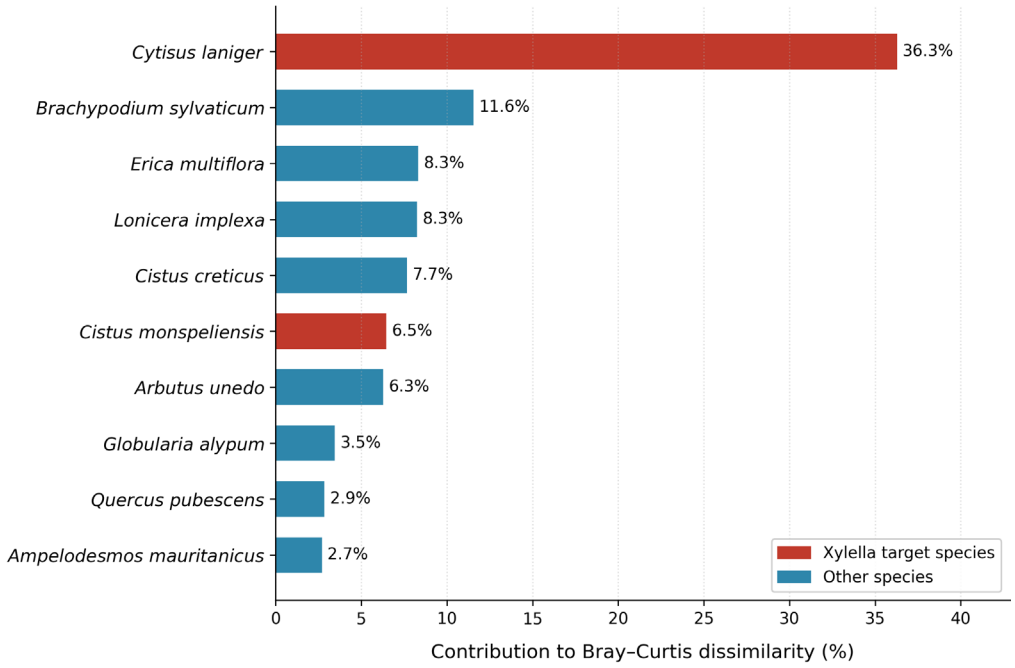

Figure 7. SIMPER analysis of species contributions to 2021–2025 Bray–Curtis dissimilarity. Bar plot showing the top ten species contributing to between-year dissimilarity. *Xylella fastidiosa* target species are highlighted in red; other species in blue.

ening effect, this modest upward deviation is best interpreted as a consequence of the structural and floristic heterogeneity of the three-habitat mosaic (H9340, H5330, H6220*), which generates higher compositional turnover across short distances than would be expected in a more physiognomically homogeneous system. In such mature sclerophyllous systems, spatial heterogeneity is driven by the gradual structural maturation of dominant taxa rather than by sharp compositional discontinuities or pioneer species invasion.

The observed richness of 90 species at 2.5 ha slightly exceeds the value predicted by the fitted model (S = 83.5) and the interval obtained from literature-based z-values for continuous Mediterranean vegetation (z = 0.15–0.25; predicted range: 73–80 species) yet remains fully coherent with SAR expectations for Mediterranean shrubland landscapes. The species richness values recorded within individual permanent plots are consistent with the fitted species-area function across the full range of sampled areas (0.0025–0.01 ha), with no systematic deviation detected at plot scale. The SAR analysis therefore serves a dual interpretative role: it validates the adequacy of the sampling design, confirming that the selected plots proportionately captured the core diversity of the 2.5 ha area, and provides a spatial framework that helps contextualize the strong compositional inertia and temporal stability observed in the multivariate analyses between 2021 and 2025.

Vegetation analysis and habitat interpretation

The hierarchical cluster analysis identified a clear vegetation composition within the investigated vegetation mosaic. The two-cluster solution defines the primary organizational pattern of the system, with a secondary partition emerging at k = 3 and clearly resolved at a Bray-Curtis dissimilarity threshold of approximately 0.54. Although cluster boundaries are gradual rather than sharp, as expected in Mediterranean sclerophyllous landscapes characterized by continuous structural transitions among vegetation phases (Whittaker 1967; Legendre and Legendre 2012), the three groupings are consistently supported by the PCoA ordination results.

Cluster A, dominated by sclerophyllous arboreal taxa (*Arbutus unedo*, *Pistacia lentiscus*, *Erica arborea*, *Quercus ilex*), corresponds structurally to the Habitat 9340 woodland matrix, whereas Cluster B, encompassing the majority of surveyed plots, reflects the shrub-grass maquis physiognomy of Habitat 5330, with *Ampelodesmos mauritanicus* and *Erica multiflora* as structural dominants. Cluster C captures a secondary level of structural heterogeneity, representing a floristically transitional subgroup characterized by increased dominance of woodland-associated species while retaining shrub physiognomy. However, habitat classification under Natura 2000 requires concordance between floristic composition and physiognomic structure (European Commission 2013): although woodland-associated species contribute substantially to this assemblage (~36% of mean total cover), canopy continuity remains incomplete and shrub dominance persists. The identified unit therefore represents a structurally mature expression within Habitat 5330, showing woodland affinity without reaching the structural threshold of Habitat 9340.

No independent therophyte-dominated assemblage emerged from the multivariate analysis, and no cluster was characterized by dominance of annual species. The very limited representation of therophytes (mean cover

below 1%) indicates that Habitat 6220* elements, while potentially present in the broader landscape matrix, do not constitute a floristically coherent unit within the sampled area. The floristic-vegetational data collected are consistent with those reported by Arrigoni and Di Tommaso (1997) for similar environmental settings on Monte Argentario.

Temporal consistency reinforces this structural interpretation: surveys conducted in 2021 and 2025 consistently grouped within the same clusters, with each plot pairing its two survey years into tight subclusters. Observed changes were restricted to compensatory dominance shifts among co-occurring woody taxa, without evidence of directional turnover. Such dynamics are characteristic of mature Mediterranean sclerophyllous systems, where structural maturation and canopy development prevail over rapid compositional replacement (Keeley and Fotheringham 2003). Overall, the convergence of hierarchical clustering, ordination analysis, and temporal stability indicates that the study area constitutes a spatially coherent and structurally mature Mediterranean shrub–woodland mosaic, whose detected differentiation reflects internal successional gradients within Habitat 5330 rather than discrete habitat entities, consistent with ecological theory describing community structure as a continuum shaped by gradual environmental and structural transitions (Whittaker 1967; McGill et al. 2006).

Temporal stability of community composition

The most striking result of the present study is the remarkable compositional stability of the monitored vegetation between 2021 and 2025. Although the PERMANOVA formally detected a significant temporal effect (p = 0.007), the associated explained variance was negligible (R^2 = 0.0039), indicating that Year accounted for less than 0.4% of total floristic variability. This outcome illustrates the well-documented distinction between statistical significance and ecological relevance in multivariate community analyses (Anderson 2017; Legendre and Legendre 2012): with permutations constrained within plots, even microscopic shifts in relative cover become detectable, yet their biological meaning remains trivial. The much larger contribution of Plot identity (R^2 = 0.995) confirms strong spatial differentiation among plots, consistent with the local environmental heterogeneity of the study area. The PCoA ordination is fully consistent with this interpretation. Paired surveys from the same plot clustered tightly in multivariate space, with trajectories so short as to be indistinguishable from sampling noise, and no consistent directional displacement was detectable along either principal axis.

SIMPER analysis corroborated this picture while adding a relevant layer of interpretation. The decomposition of the negligible interannual dissimilarity revealed that *Cytisus laniger* alone accounted for 36.3% of between-year floristic change, a disproportionate contribution for a single taxon in an otherwise stable community, directly reflecting its significant cover increase documented in the Target dynamics section. This result confirms that the minimal compositional shift detected between 2021 and 2025 was not distributed randomly across the flora but was concentrated in the most dynamically active Xfm ST87 target species. The remaining target species contributed marginally to interannual dissimilarity, consistent with their cover stability over the monitoring period. Together, these analyses paint a coherent picture of strong structural and compositional inertia, a hallmark of mature, stress-tolerant Mediterranean woody vegetation (Blondel and Aronson 1999; Lloret et al. 2012), while identifying *Cytisus laniger* as the floristic element most deserving of attention in future resurveys.

Such structural inertia is not merely a passive property of established vegetation. Mediterranean woody communities, and maquis formations in particular, are known to exhibit considerable buffering capacity against moderate disturbance through resprouting, clonal growth, and the persistent soil seed bank (Pausas et al. 2004; Verdú and Pausas 2007). The absence of any detectable floristic collapse over the monitoring period therefore does not preclude the ongoing presence of Xfm ST87 in the study area, but indicates that the plant community as a whole has not yet experienced measurable phytopathological impact at the community scale. Landscape-level effects of *Xylella fastidiosa* subsp. *pauca* on olive groves in Apulia have been documented only after a decade or more of progressive symptom development (Saponari et al. 2019; Boscia et al. 2017), suggesting that the period examined here may be insufficient to detect early-stage floristic shifts in species with slow demographic turnover such as the woody taxa dominating this study area.

Alpha-diversity patterns: stability with a subtle evenness shift

Alpha-diversity results are consistent with the overall picture of community stability, while revealing subtle internal shifts in species dominance. Species richness remained perfectly stable between the two survey campaigns (W = 5.0, p = 0.750), indicating that no local extinctions or colonizations occurred within the permanent plots, a result consistent with the conserved floristic matrix documented by multivariate analyses.

While the Shannon Diversity Index displayed a slight numerical fluctuation between the two survey campaigns (from 1.690 to 1.711; uncorrected p = 0.043), alongside marginal positive trends for Simpson's Index (1–D) and Pielou's Evenness (J'), the absolute magnitude of these shifts was ecologically negligible (delta = +0.021 for Shannon). Thus, the overall pattern is best interpreted as stable: the community did not genuinely diversify, but the distribution of relative abundances shifted very slightly towards greater evenness.

This subtle shift in uniformity, in the absence of any change in species richness, is consistent with a partial redistribution of cover between species rather than compositional substitution. For example, the slight decline in cover dominance of *Ampelodesmos mauritanicus* is offset by the increase in subdominant species. Such minor fluctuations in diversity metrics without changes in species richness have been documented in Mediterranean shrublands undergoing post-disturbance recovery or interannual climatic variability (De Cáceres et al. 2015; Lloret et al. 2012), and do not necessarily imply any directional ecological trend.

Target dynamics

The analysis of the Xfm ST87 target species recorded in the permanent plots (*Cytisus laniger*, *Spartium junceum*, *Rhamnus alaternus* and *Cistus monspeliensis*) constitutes perhaps the most ecologically significant component of the present study, as it directly addresses the primary concern motivating the monitoring design.

None of the target species showed a decline in cover over the study period. *Spartium junceum* and *Rhamnus alaternus* were perfectly stable across all twelve plots ($\Delta = 0$ in all cases). *Cistus monspeliensis* was largely stable across plots ($\Delta = 0$ in 10 out of 12 plots), with only minor and non-directional cover fluctuations (contributing 6.5% to interannual dissimilarity). *Cytisus laniger*, one of the *Xylella fastidiosa* subsp. *multiplex* ST87 host species reported in the Mediterranean maquis of central Italy (EFSA 2026; Falsini et al. 2025), showed not a decline but a statistically significant increase in mean cover, rising from 6.37% in 2021 to 10.97% in 2025 ($W = 0$, $p = 0.0078$), with cover increasing in eight out of twelve plots and remaining unchanged in the remaining four. This result is unambiguous and counter-intuitive from a strictly pathological perspective.

Several non-mutually exclusive interpretations can be advanced. First, the absence of visible decline in *C. laniger* may reflect the early and sub-symptomatic phase of infection, during which bacterial colonization progresses through the xylem vessels without yet triggering the severe water stress and scorching symptoms that characterize advanced disease stages (Saponari et al. 2013; Sicard et al. 2018). Second, it is possible that the local populations of *C. laniger* exhibit a degree of tolerance or partial resistance to the bacterium, as has been documented for certain genotypes of *Xylella* hosts in other contexts (Velasco-Amo et al. 2020). Third, the observed cover increase may simply reflect the intrinsic growth dynamics of a fast-growing, resprouting leguminous shrub, whose canopy expansion between the two survey campaigns is well within the range of natural interannual variability in Mediterranean shrublands, independent of any pathological process. Finally, the monitoring window may simply be insufficient to detect early-stage population declines in a perennial resprouting shrub, whose vegetative growth can mask underlying root and xylem damage for several growing seasons before external symptoms become visible (Saponari et al. 2019).

Regardless of the mechanism involved, the absence of vegetation variation over the 2021–2025 period is an important baseline finding. It provides a reference against which future resurveys, particularly if extended to a ten-year horizon, can detect the onset of plant landscape change.

Conclusions

This study offers one of the first assessments of how Mediterranean maquis and garrigue vegetation responds to the presence of *Xylella fastidiosa* subsp. *multiplex* ST87, based on a sampling design whose adequacy was independently confirmed by the species-area analysis. Between 2021 and 2025, the plant communities of Monte Argentario's Valle della Soda proved remarkably stable across all three Natura 2000 habitats monitored, with no species lost and no sign of directional change, a result that fits well with what is known about the resilience of mature Mediterranean shrub vegetation, which can absorb moderate disturbance through resprouting, clonal growth and a persistent soil seed bank. The one exception was *Cytisus laniger*, whose cover increased significantly and consistently enough to make it the species to watch in future surveys. Because the incubation period of *Xylella fastidiosa* can vary enormously, from a few months to several years depending on the host, these five years are best treated as an early, pre-symptomatic baseline rather than proof that the vegetation is unaffected. Only monitoring extended over a longer period, ideally a decade or more, will tell us whether and how this pathogen eventually leaves a mark on the landscape.

References

Agisoft LLC (2021) Agisoft Metashape Professional, version 1.7.5. Agisoft LLC, St. Petersburg, Russia.

Anderson MJ (2001) A new method for non-parametric multivariate analysis of variance. Austral Ecology 26: 32–46. https://doi.org/10.1111/j.1442-9993.2001.01070.pp.x

Anderson MJ (2006) Distance-based tests for homogeneity of multivariate dispersions. Biometrics 62: 245–253. https://doi.org/10.1111/j.1541-0420.2005.00440.x

Anderson MJ (2017) Permutational multivariate analysis of variance (PERMANOVA). In: Balakrishnan N, Colton T, Everitt B, Piegorsch W, Ruggeri F, Teugels JL (Eds) Wiley StatsRef: Statistics Reference Online. https://doi.org/10.1002/9781118445112.stat07841

Arrhenius O (1921) Species and area. Journal of Ecology 9: 95–99. https://doi.org/10.2307/2255763

Arrigoni PV, Di Tommaso PL (1997) La vegetazione del Monte Argentario (Toscana meridionale). Parlatorea 2: 5–38.

Baldini RM (1995) Flora vascolare del Monte Argentario (Arcipelago Toscano). Webbia 50(1): 67–191. https://doi.org/10.1080/00837792.1995.10670598

Bartolucci F, Peruzzi L, Galasso G, Alessandrini A, Ardenghi NMG, … Conti F (2024) A second update to the checklist of the vascular flora native to Italy. Plant Biosystems 158(2): 219–296. https://doi.org/10.1080/11263504.2024.2320126

Bertacchi A (2022) UAVs technology as a complementary tool in post-fire vegetation recovery surveys in Mediterranean fire-prone forests. Forests 13: 1009. https://doi.org/10.3390/f13071009

Bertacchi A, Orazi D, Ercolini L (2025) The ledge plant communities in a limestone cave of the Apuan area: identification and survey by UAV technology. Italian Botanist 20: 9–22. https://doi.org/10.3897/italianbotanist.20.145009

Bertacchi A, Orazi D, Bedini S, Lombardi T (2026) Spatial Analysis and Spread Monitoring of a Population of *Juniperus macrocarpa* Sm. Across Coastal Dune Systems in Northern Tuscany (Italy). Biology 15(3): 278. https://doi.org/10.3390/biology15030278

Biondi E, Blasi C, Burrascano S, Casavecchia S, Copiz R, … Zivkovic L (2010) Manuale italiano di interpretazione degli habitat della Direttiva 92/43/CEE. Società Botanica Italiana, Ministero dell'Ambiente e della Tutela del Territorio e del Mare, DPN. http://vnr.unipg.it/habitat

Biondi E, Blasi C, Allegrezza M, Anzellotti I, Azzella MM, … Zivkovic L (2014) Plant communities of Italy: the VegItaly database. Plant Biosystems 148: 430–443.

Blasi C, Marignani M, Copiz R, Fipaldini M, Del Vico E (2010) Important plant areas: using plant diversity to identify key sites for conservation in Italy. Plant Biosystems 144: 298–306.

Blondel J, Aronson J (1999) Biology and wildlife of the Mediterranean region. Oxford University Press, Oxford.

Boscia D, Altamura G, Saponari M, Tavano D, Zicca S, … Cornara D (2017) Incidence of *Xylella fastidiosa* subsp. *pauca* in olive trees and other host plants in areas under containment and delay strategies in Apulia, Italy. Phytopathologia Mediterranea 56: 605–613.

Burbank LP, Roper MC (2021) Microbe profile: *Xylella fastidiosa*–a devastating agricultural pathogen with an endophytic lifestyle. Microbiology 167(10): 001091. https://doi.org/10.1099/mic.0.001091

Burdon JJ, Thrall PH, Ericson AL (2006) The current and future dynamics of disease in plant communities. Annual Review of Phytopathology 44: 19–39. https://doi.org/10.1146/annurev.phyto.43.040204.140238

Carmignani L, Lazzarotto A (2004) Carta geologica della Toscana (scala 1:250.000). Università di Siena, Dipartimento Scienze della Terra, Centro di GeoTecnologie, Regione Toscana, Firenze.

Chianucci F, Disperati L, Guzzi D, Bianchini D, Nardino V, … Corona P (2016) Estimation of canopy attributes in beech forests using true colour digital images from a small fixed-wing UAV. International Journal of Applied Earth Observation and Geoinformation 47: 60–68. https://doi.org/10.1016/j.jag.2015.12.005

Clarke KR (1993) Non-parametric multivariate analyses of changes in community structure. Australian Journal of Ecology 18: 117–143. https://doi.org/10.1111/j.1442-9993.1993.tb00438.x

D'Antraccoli M, Peruzzi L, Conti F, Bartolucci F (2024) Floristic richness in a Mediterranean hotspot: a journey across Italy. Plants 13: 12. https://doi.org/10.3390/plants13010012

De Cáceres M, Chytrý M, Agrillo E, Attorre F, Botta-Dukát Z, … Wiser SK (2015) A comparative framework for broad-scale plot-based vegetation classification. Applied Vegetation Science 18: 543–560. https://doi.org/10.1111/avsc.12179

de Castro AI, Shi Y, Maja JM, Peña JM (2021) UAVs for vegetation monitoring: overview and recent scientific contributions. Remote Sensing 13: 2139. https://doi.org/10.3390/rs13112139

Denancé N, Legendre B, Briand M, Olivier V, De Boisseson C, … Belin S (2017) Several subspecies and sequence types are associated with the emergence of *Xylella fastidiosa* in natural settings in France. Plant Pathology 66: 1054–1064. https://doi.org/10.1111/ppa.12695

Desprez-Loustau ML, Balci Y, Cornara D, Gonthier P, Robin C, Jacques MA (2020) Is *Xylella fastidiosa* a serious threat to European forests? Forestry 94: 1–17. https://doi.org/10.1093/forestry/cpaa029

DJI (2024) DJI Fly. SZ DJI Technology Co., Ltd., Shenzhen, China.

Drakare S, Lennon JJ, Hillebrand H (2006) The imprint of the geographical, evolutionary and ecological context on species–area relationships. Ecology Letters 9: 215–227. https://doi.org/10.1111/j.1461-0248.2005.00848.x

Duarte A, Borralho N, Cabral P, Caetano M (2022) Recent advances in forest insect pests and diseases monitoring using UAV-based data: a systematic review. Forests 13(6): 911. https://doi.org/10.3390/f13060911

European Environment Agency (2017) Biogeographical regions in Europe. https://www.eea.europa.eu/data-and-maps/figures/biogeographical-regions-in-europe-2 [Accessed 25 March 2026]

EFSA [European Food Safety Authority] (2019) Update of the scientific opinion on the risks to plant health posed by *Xylella fastidiosa* in the EU territory. EFSA Journal 17: 5665. https://doi.org/10.2903/j.efsa.2019.5665

EFSA [European Food Safety Authority] (2023) Pest survey card on *Xylella fastidiosa*. https://efsa.europa.eu/plants/planthealth/monitoring/surveillance/xylella-fastidiosa [Accessed 25 March 2026]

EFSA [European Food Safety Authority] [Cavalieri V, Fasanelli E, Furnari G, Gibin D, Gutierrez Linares A, … Stancanelli G] (2026) Update of the *Xylella* spp. host plant database – Systematic literature search up to 31 December 2025. EFSA Journal 24(6): e10147. https://doi.org/10.2903/j.efsa.2026.10147

EPPO [European and Mediterranean Plant Protection Organization] (2020) PM 3/81 (2) Inspection of consignments for *Xylella fastidiosa*. EPPO Bulletin 50(3): 401–414. https://doi.org/10.1111/epp.12690

EPPO [European and Mediterranean Plant Protection Organization] (2023) PM 7/24 (5) *Xylella fastidiosa*. EPPO Bulletin 53: 205–276. https://doi.org/10.1111/epp.12923

European Commission (2013) Interpretation manual of European Union habitats – EUR 28. European Commission DG Environment, Brussels.

Falsini S, Campigli S, Faraoni P, Tani C, Rech V, … Marchi G (2025) Observations on *Rhamnus alaternus* naturally infected by *Xylella fastidiosa* subsp. *multiplex* ST87 in the Mediterranean maquis of Monte Argentario (Tuscany, Italy). Plant Pathology 74(6): 1813–1829. https://doi.org/10.1111/ppa.14129

Fornace KM, Drakeley CJ, William T, Espino F, Cox J (2014) Mapping infectious disease landscapes: unmanned aerial vehicles and epidemiology. Trends in Parasitology 30(11): 514–519. https://doi.org/10.1016/j.pt.2014.09.001

Gallet F, Bioret B, Fichaut J, Sawtschuk J (2010) La phytosociologie, outil pertinent pour le suivi de la restauration écologique? Revue Forestière Française 62(3/4): 409–416. https://doi.org/10.4267/2042/38954

Gilbert GS (2002) Evolutionary ecology of plant diseases in natural ecosystems. Annual Review of Phytopathology 40: 13–43. https://doi.org/10.1146/annurev.phyto.40.021202.110417

Godínez-Alvarez H, Herrick JE, Mattocks M, Toledo D, Van Zee J (2009) Comparison of three vegetation monitoring methods: their relative utility for ecological assessment and monitoring. Ecological Indicators 9(5): 1001–1008. https://doi.org/10.1016/j.ecolind.2008.11.011

ISPRA (2016) Manuali per il monitoraggio degli habitat di interesse comunitario (Direttiva 92/43/CEE). Manuale ISPRA 142/2016.

Keeley JE, Fotheringham CJ (2003) Species-area relationships in Mediterranean-climate plant communities. Journal of Biogeography 30: 1629–1657. https://doi.org/10.1046/j.1365-2699.2003.00950.x

Kent M (2012) Vegetation description and data analysis: a practical approach, 2nd edn. Wiley-Blackwell, Oxford.

Konatowska M, Rutkowski P (2019) Phytosociology — a useful tool for the assessment of past and future human impacts on plants and forest ecosystems. Journal of Biosciences and Medicines 7: 154–163. https://doi.org/10.4236/jbm.2019.711014

Köppen W (1936) Das geographische System der Klimate. In: Köppen W, Geiger R (Eds) Handbuch der Klimatologie, Vol. 1. Borntraeger, Berlin.

Kouadio L, El Jarroudi M, Belabess Z, Laasli SE, Roni MZK, … Lahlali R (2023) A review on UAV-based applications for plant disease detection and monitoring. Remote Sensing 15: 4273. https://doi.org/10.3390/rs15174273

Lazzarotto A, Mazzanti R, Mazzoncini F (1964) Geologia del Promontorio Argentario (Grosseto) e del Promontorio del Franco (Isola del Giglio – Grosseto). Bollettino della Società Geologica Italiana 83(2): 1–124.

Legendre P, Gallagher ED (2001) Ecologically meaningful transformations for ordination of species data. Oecologia 129: 271–280. https://doi.org/10.1007/s004420100716

Legendre P, Legendre L (2012) Numerical ecology, 3rd edn. Elsevier, Amsterdam.

Lengyel S, Déri E, Varga Z, Horváth R, Tóthmérész B, … Reiter K (2008) Habitat monitoring in Europe: a description of current practices. Biodiversity and Conservation 17: 3327–3339. https://doi.org/10.1007/s10531-008-9395-3

Lloret F, Médail F, Brundu G, Camarda I, Moragues E, … Hulme PE (2005) Species attributes and invasion success by alien plants on Mediterranean islands. Journal of Ecology 93: 512–520. https://doi.org/10.1111/j.1365-2745.2005.00979.x

Lloret F, Escudero A, Iriondo JM, Martínez-Vilalta J, Valladares F (2012) Extreme climatic events and vegetation: the role of stabilizing processes. Global Change Biology 18: 797–805. https://doi.org/10.1111/j.1365-2486.2011.02624.x

Marchi G, Rizzo D, Ranaldi F, Ghelardini L, Ricciolini M, … Surico G (2018) First detection of *Xylella fastidiosa* subsp. *multiplex* DNA in Tuscany (Italy). Phytopathologia Mediterranea 57(3): 363–364.

Martellos S, Bartolucci F, Conti F, Galasso G, Moro A, … Nimis PL (2020) FlorItaly – the portal to the flora of Italy. PhytoKeys 156: 55–71. https://doi.org/10.3897/phytokeys.156.54023

McGill BJ, Enquist BJ, Weiher E, Westoby M (2006) Rebuilding community ecology from functional traits. Trends in Ecology and Evolution 21: 178–185. https://doi.org/10.1016/j.tree.2006.02.002

Mueller-Dombois D, Ellenberg H (1974) Aims and methods of vegetation ecology. John Wiley and Sons, New York.

Oksanen J, Blanchet FG, Friendly M, Kindt R, Legendre P, … Wagner H (2023) vegan: community ecology package. R package version 2.6-4. https://CRAN.R-project.org/package=vegan

Pausas JG, Bradstock RA, Keith DA, Keeley JE (2004) Plant functional traits in relation to fire in crown-fire ecosystems. Ecology 85: 1085–1100. https://doi.org/10.1890/02-4094

Perroy RL, Meier P, Collier E, Hughes MA, Brill E, … Keith LM (2022) Aerial Branch sampling to detect forest pathogens. Drones 6(10): 275. https://doi.org/10.3390/drones6100275

Pesaresi S, Biondi E, Casavecchia S (2017) Bioclimates of Italy. Journal of Maps 13(2): 955–960. https://doi.org/10.1080/17445647.2017.1413017

Pielou EC (1966) The measurement of diversity in different types of biological collections. Journal of Theoretical Biology 13: 131–144. https://doi.org/10.1016/0022-5193(66)90013-0

Pignatti S, Guarino R, La Rosa M (2017–2019) Flora d'Italia, 2nd edn. Edagricole – Edizioni Agricole di New Business Media, Bologna.

QGIS Development Team (2024) QGIS geographic information system, version 3.42.0. Open Source Geospatial Foundation. https://www.qgis.org

Quattrini G, Pesaresi S, Lucchetti L, Hofmann N, Saiter F, … Casavecchia S (2025) Standardised drone procedures for phytosociological data collection. Applied Vegetation Science 28(2): e70032. https://doi.org/10.1111/avsc.70032

R Core Team (2024) R: a language and environment for statistical computing. R Foundation for Statistical Computing, Vienna. https://www.R-project.org/

Raunkiaer CC (1934) The life forms of plants and statistical plant geography. Oxford University Press, Oxford.

Rosenzweig ML (1995) Species diversity in space and time. Cambridge University Press, Cambridge. https://doi.org/10.1017/cbo9780511623387

Saponari M, Boscia D, Nigro F, Martelli GP (2013) Identification of DNA sequences related to *Xylella fastidiosa* in oleander, almond and olive trees exhibiting leaf scorch symptoms in Apulia (southern Italy). Journal of Plant Pathology 95: 668.

Saponari M, Giampetruzzi A, Loconsole G, Boscia D, Saldarelli P (2019) *Xylella fastidiosa* in olive in Apulia: where we stand. Phytopathology 109: 175–186. https://doi.org/10.1094/phyto-08-18-0319-fi

Shannon CE (1948) A mathematical theory of communication. The Bell System Technical Journal 27(3): 379–423. https://doi.org/10.1002/j.1538-7305.1948.tb01338.x

Scortichini M (2026) Assessing the potential for modifying certain eradication measures for *Xylella fastidiosa* subsp. *pauca* in olive groves of Apulia (Italy). Agriculture 16(2): 145. https://doi.org/10.3390/agriculture16020145

SFR (2026) Servizio Fitosanitario Regionale Toscana. https://fitosirt.regione.toscana.it/ [Accessed on 14 February 2026]

Sicard A, Zeilinger AR, Vanhove M, Schartel TE, Beal DJ, … Almeida RPP (2018) *Xylella fastidiosa*: insights into an emerging plant pathogen. Annual Review of Phytopathology 56: 181–202. https://doi.org/10.1146/annurev-phyto-080417-045849

Simpson EH (1949) Measurement of diversity. Nature 163: 688. https://doi.org/10.1038/163688a0

Strumia S, Buonanno M, Aronne G, Santo A, Santangelo A (2020) Monitoring of plant species and communities on coastal cliffs: is the use of unmanned aerial vehicles suitable? Diversity 12: 149. https://doi.org/10.3390/d12040149

Tjørve E (2009) Shapes and functions of species-area curves (II): a review of new models and parameterizations. Journal of Biogeography 36: 1435–1445. https://doi.org/10.1111/j.1365-2699.2009.02101.x

Tjørve E, Tjørve KM (2017) Species–area relationship. In: eLS. John Wiley and Sons, Chichester. https://doi.org/10.1002/9780470015902.a0026330

Turner W, Spector S, Gardiner N, Fladeland M, Sterling E, Steininger M (2003) Remote sensing for biodiversity science and conservation. Trends in Ecology and Evolution 18: 306–314. https://doi.org/10.1016/s0169-5347(03)00070-3

Vacek S, Černý T, Vacek Z, Podrázský V, Mikeska M, Králíček I (2017) Long-term changes in vegetation and site conditions in beech and spruce forests of lower mountain ranges of Central Europe. Forest Ecology and Management 398: 75–90. https://doi.org/10.1016/j.foreco.2017.05.001

Velasco-Amo MP, Landa BB, Pizarro-Tobías P, Trapero-Casas JL, Bejarano ER, … Navas-Cortés JA (2020) Resident bacterial microbiota in *Olea europaea* L. and its relationship with susceptibility or tolerance to *Xylella fastidiosa* subsp. *pauca*. Frontiers in Plant Science 11: 1168.

Vennin S, Montpied P, Behr P, Thimonier A, Dupouey JL (2025) Mechanisation of forest operations drives long-term changes in plant communities. Forest Ecology and Management 585: 122562. https://doi.org/10.1016/j.foreco.2025.122562

Verdú M, Pausas JG (2007) Fire drives phylogenetic clustering in Mediterranean Basin woody plant communities. Journal of Ecology 95: 1316–1323. https://doi.org/10.1111/j.1365-2745.2007.01300.x

Viciani D, Dell'Olmo L, Foggi B, Ferretti G, Lastrucci L, Gennai M (2018) Natura 2000 habitat of Mt. Argentario promontory (southern Tuscany, Italy). Journal of Maps 14(2): 447–454. https://doi.org/10.1080/17445647.2018.1489903

Whittaker RH (1967) Gradient analysis of vegetation. Biological Reviews 42: 207–264. https://doi.org/10.1111/j.1469-185x.1967.tb01419.x

Additional information

Conflict of interest

The authors have declared that no competing interests exist.

Ethical statement

No ethical statement was reported.

Artificial Intelligence (AI) use

AI-assisted language tools were used during the preparation of this manuscript for grammar checking and text refinement. All scientific content, data analysis, interpretation, and conclusions are entirely the responsibility of the authors.

Funding

This work was supported by Regione Toscana, Servizio Fitosanitario Regionale (SFR).

Author contributions

Conceptualization: AB, TL; Data curation: AB, TL, DO, SC, GM; Formal analysis: AB, TL, DO; Funding acquisition: LD; Methodology: AB, GM; Resources: LD; Visualization: DO, TL; Writing—original draft: AB, TL; Writing—review and editing: all authors.

Author ORCIDs

A. Bertacchi https://orcid.org/0000-0002-3276-3876
D. Orazi https://orcid.org/0009-0000-6591-8427
S. Campigli https://orcid.org/0000-0001-7231-535X
G. Marchi https://orcid.org/0000-0002-2937-3500
T. Lombardi https://orcid.org/0000-0003-0427-1820

Data availability

The vegetation dataset supporting the results of this study is available as Supplementary material (Suppl. material 1: tables S1–S3, figs S1–S3).

Supplementary material 1

Supplementary figures S1–S3 and tables S1–S3

Authors: Andrea Bertacchi, Diego Orazi, Sara Campigli, Guido Marchi, Lorenzo Drosera, Tiziana Lombardi

Data type: zip

Copyright notice: This dataset is made available under the Open Database License (http://opendatacommons.org/licenses/odbl/1.0). The Open Database License (ODbL) is a license agreement intended to allow users to freely share, modify, and use this Dataset while maintaining this same freedom for others, provided that the original source and author(s) are credited.

Link: https://doi.org/10.3897/ved.197154.suppl1